

**Asymmetric interfacial Ru single-atom sites and nanoparticles for
promoting hydrogen evolution reaction in a wide pH range**

Chaoqun Wang^{#, ab}, Yingping Li^{#, b}, Han Xiao,^c Shi Chen,^b Mingyue Wang,^b Mingfu
Ye,^b Hui Miao,^{*a} Binbin Jiang^{*c} and Konglin Wu^{*bd}

^a *Biomass Conversion and Pollution Control Engineering Technology Research Center of Anhui Province, School of Chemistry and Materials Engineering, Fuyang Normal University, Fuyang 236037, China*

^b *Institute of Clean Energy and Advanced Nanocatalysis (iClean), School of Chemistry and Chemical Engineering, Anhui University of Technology, Maanshan 243032, China*

^c *Anhui Provincial Key Laboratory of Advanced Catalysis and Energy Materials, School of Chemistry and Chemical Engineering, Anqing Normal University, Anqing 246001, China*

^d *State Key Laboratory of Heavy Oil Processing, China University of Petroleum (East China), Qingdao 266580, China*

[#] *These authors contributed equally to this work.*

Corresponding authors:

huimiao@mail.ahnu.edu.cn (H. Miao);

klwuchem@ahut.edu.cn (K. Wu);

jiangbb@aqnu.edu.cn (B. Jiang)

1. Materials and Methods

1.1 Chemical reagents

CM-Cellulose Na Salt was purchased from Shanghai Chemical Reagent Company. Melamine ($C_3H_6N_6$), ruthenium nitrate ($Ru(NO)(NO_3)_3$), and Nafion solution (5 wt%) were purchased from Alfa Aesar Chemical Co., Ltd. Sodium phytate ($C_6H_6Na_{12}O_{24}P_6$) and disodium hydrogen phosphate ($Na_2H_2PO_4 \cdot 12H_2O$) were purchased from Shanghai Titan Scientific Co., Ltd. Commercial Pt/C catalyst (5 wt%) was purchased from Beijing Inno Chem Science & Technology Co., Ltd. Sodium dihydrogen phosphate ($NaH_2PO_4 \cdot 2H_2O$) was purchased from Shanghai Xinhua Chemical Factory. Sodium hydroxide (NaOH), potassium hydroxide (KOH), and sulfuric acid (H_2SO_4) were purchased from Kunshan Jincheng Reagent Co., Ltd. Anhydrous ethanol (C_2H_5OH , 99.7%) was purchased from Sinopharm Chemical Reagent Co., Ltd. High-purity argon (Ar, 99.999%), high-purity oxygen (O_2 , 99.999%), and high-purity nitrogen (N_2 , 99.999%) were purchased from Nanjing Specialty Gas Co., Ltd. All chemicals were used without any further purification.

1.2 Synthesis of Ru loaded nitrogen and phosphorus co-doped carbon materials

CM-Cellulose Na salt (1.0 g), $C_3H_6N_6$ (1.0 g), $C_6H_6Na_{12}O_{24}P_6$ (0.8 g), and $Ru(NO)(NO_3)_3$ (40mg, 80 mg, 120 mg or 140 mg) were added to 20 mL of deionized water and ultrasonically stirred for 30 minutes. The solution mixture was heated at 60 °C to form a yellow sol and freeze-dried to form a yellow gel. The yellow gel was heated under a nitrogen atmosphere at a rate of 2 °C min^{-1} to 550 °C, held for 2 hours, and then further heated at the same rate to temperature 700 °C for 3 hours, and cooled to room temperature to collect the product. The achieved composite was denoted as $Ru_{1+NPS}/NPC-1$, Ru_{1+NPS}/NPC , $Ru_{1+NPS}/NPC-2$ and $Ru_{1+NPS}/NPC-3$, respectively.

1.3 Synthesis of Ru loaded nitrogen-doped carbon materials

1 g of CM-Cellulose Na Salt, 1 g of $C_3H_6N_6$, and 80 mg of $Ru(NO)(NO_3)_3$ were added to 20 mL of deionized water and ultrasonically stirred for 30 minutes. The solution mixture was heated at 60 °C to form a yellow sol and freeze-dried to form a yellow gel. The product was heated to 700 °C using the same heating procedure, held for 3 hours, cooled to room temperature, and collected. The product was named Ru/NC.

1.3 Synthesis of Ru loaded phosphorus-doped carbon materials

1 g of CM-Cellulose Na Salt, 0.8 g of $C_6H_6Na_{12}O_{24}P_6$, and 80 mg of $Ru(NO)(NO_3)_3$ were added

to 20 mL of deionized water and ultrasonically stirred for 30 minutes. The solution mixture was heated at 60 °C to form a yellow sol and freeze-dried to form a yellow gel. The product was heated to 700 °C using the same heating procedure, held for 3 hours, cooled to room temperature, and collected. The product was named Ru/PC.

1.4 Synthesis of Ru loaded carbon materials

1 g of CM-Cellulose Na Salt and 80 mg of Ru(NO)(NO₃)₃ were added to 20 mL of deionized water and ultrasonically stirred for 30 minutes. The solution mixture was heated at 60 °C to form a yellow sol and freeze-dried to form a yellow gel. The gel was heated under a nitrogen atmosphere at 2 °C min⁻¹ to 550 °C, held for 2 hours, then heated at the same rate to 700 °C, held for 3 hours, and the product was collected. The product was named Ru/C.

1.5 Microstructural and chemical characterization

Transmission electron microscopy (TEM, Hitachi HT7800), scanning electron microscopy (SEM, Hitachi S-4800), and high-angle annular dark-field scanning transmission electron microscopy (HAADF-STEM, FEI Titan Theims Z) were used to characterize the external features and elemental distribution of the material. X-ray diffraction (XRD, Rigku, Ulitma IV) was employed to determine the phase structure of catalysts. The degree of graphitization of the material was investigated by the Raman spectra. X-ray photoelectron spectroscopy (XPS, Thermo Scientific K-Alpha) was used to analyze the chemical composition and valence state changes of elements in the sample. The Brunauer–Emmett–Teller (BET, Micromeritics ASAP 2460) analyzer was used to measure the specific surface area, pore volume, and pore size distribution of the material. The Ru contents in all samples were determined by ICP-OES (Agilent 5110(OES)). The X-ray absorption fine structure spectra Ru K-edge were collected at 44A beamline of National Synchrotron Radiation Research Center (NSRRC) Taiwan, and the data were collected in fluorescence mode using a Lytle detector while the corresponding reference sample were collected in transmission mode. The authors would like to thank Guilin Zhu from Melab Scientific Research Platform (www.micetech.cn) for the aberration-corrected HAADF-STEM analysis. The authors would like to thank Shiyanjia (<https://www.shiyanjia.com/>) for the XPS and ICP-OES analysis.

2. Electrochemical performance test

Pre-treatment of the working electrode: The L-shaped glassy carbon electrode (GCE, diameter 5 mm) used in the electrochemical workstation was carefully polished on chamois leather coated

with micron-sized Al₂O₃. Modification of the working electrode: 5 mg of the catalyst to be tested was mixed with 50 μL of Nafion (5 wt%) and added to a solution of 500 μL water and 480 μL ethanol. The mixture was ultrasonicated for at least 30 minutes. A well-dispersed catalytic ink (20 μL) was drop-cast in four steps onto the polished glassy carbon electrode and dried under an infrared lamp.

Electrochemical testing employed a standard three-electrode system: The electrolytes used were 1.0 M KOH, 0.5 M H₂SO₄, and 1.0 M PBS. The working electrode was an L-shaped glassy carbon electrode, the counter electrode was a carbon rod, and the reference electrode was Ag/AgCl. All potentials in the study were converted to reversible hydrogen electrode (RHE) potentials using the Nernst equation: $E_{\text{RHE}} = E_{\text{Ag/AgCl}} + 0.197 + 0.059 \text{ pH}$. In this experiment, the HER performance were recorded by linear scanning voltammetry at a scan rate of 5 mV s⁻¹ with 90% *iR* correction in 1.0 M KOH, 0.5 M H₂SO₄ and 1.0 M PBS, respectively. The Tafel plot is obtained from linear sweep voltammetry with the following formula: $\eta = a + \text{blog}(j/j_0)^{S1}$. The double-layer capacitance (*C_{dl}*) was estimated by cyclic voltammetry (CV). The electrochemical impedance spectroscopy (EIS) was performed with a frequency range of 0.1 Hz to 100 kHz and an amplitude of 5 mV. The stability of catalysts in electrocatalytic hydrogen evolution. Here, the electrochemical stability of the material was tested using the *i-t* method at about 20 mA cm⁻² over 20 h.

The ultra-long time stability test as follows: A three-electrode system is adopted. The Ru_{1+NPs}/NPC catalyst is prepared into ink droplets and placed on a 1*1 cm² carbon paper (with a catalyst loading of 1 mg cm⁻²) as the working electrode, the graphite rod as counter electrode, and the Hg/HgO electrode as reference electrode. The volume of the electrolytic cell is a 150 mL glass electrolytic cell, and the electrolyte is a 1 M KOH solution saturated with oxygen. The ultra-long stability of the catalyst for 100 h was carried out using chronoamperometry mode (Chenhua 660E electrochemical workstation) under initial current density is 22.6 mA cm⁻².

Reference:

S1. A. Ali and P. K. Shen, *Electrochem. Energy Rev.*, 2020, **3**, 370-394.

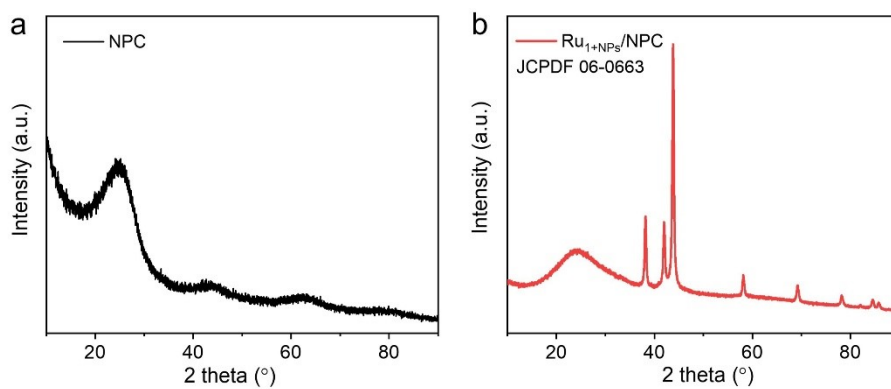


Fig. S1 XRD pattern of (a) NPC and (b) Ru_{1+NP8}/NPC.

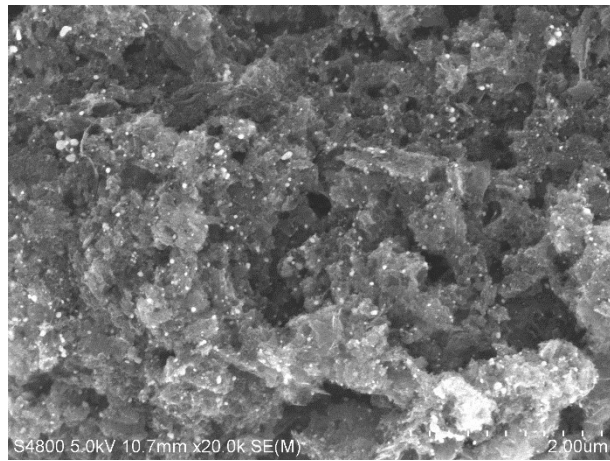


Fig. S2 SEM image of Ru₁+NPs/NPC.

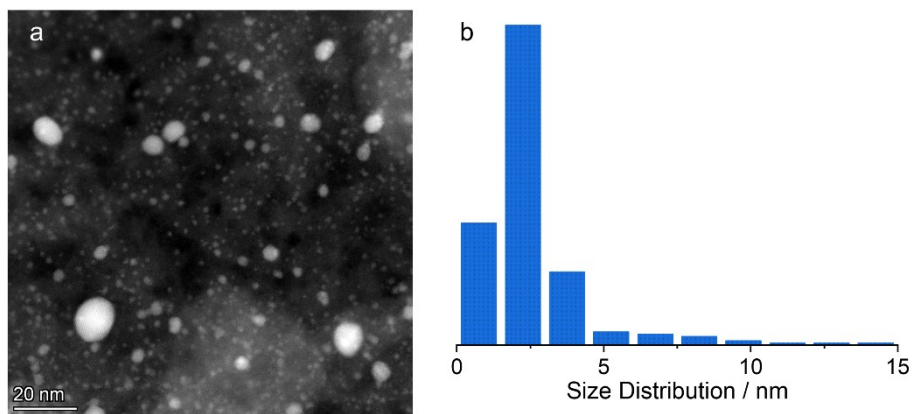


Fig. S3 (a) AC-HRTEM and (b) size distribution of Ru_{1+NP₆}/NPC surface.

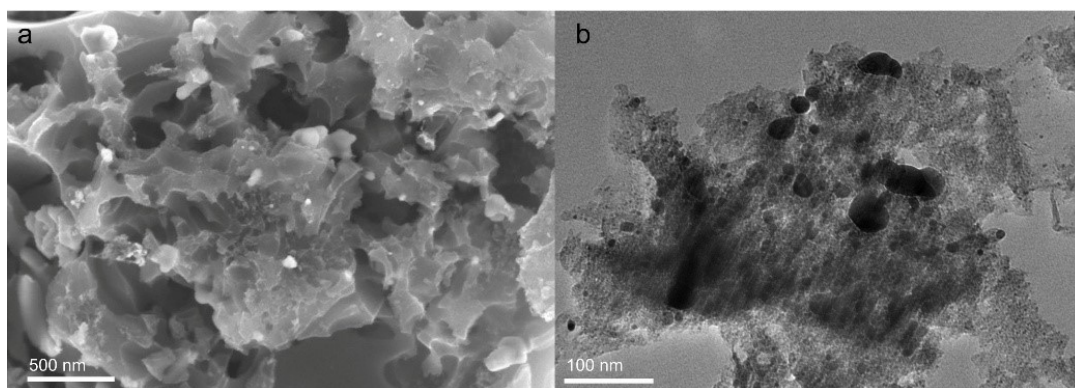


Fig. S4 (a) SEM and **(b)** TEM images of Ru/C.

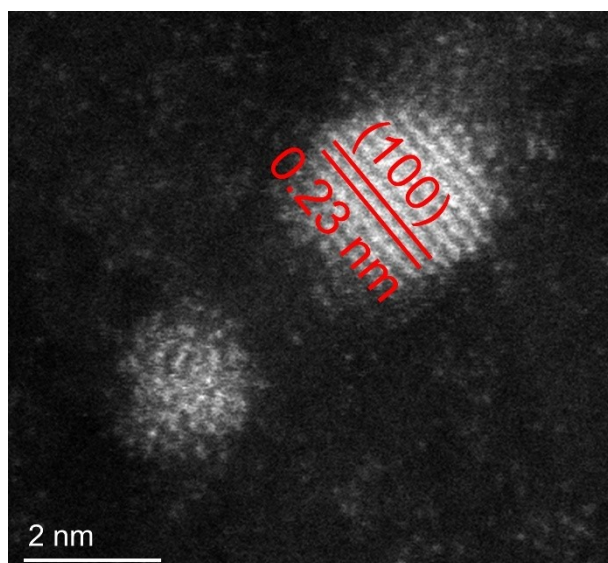


Fig. S5 HRTEM of Ru_{1+NP8}/NPC.

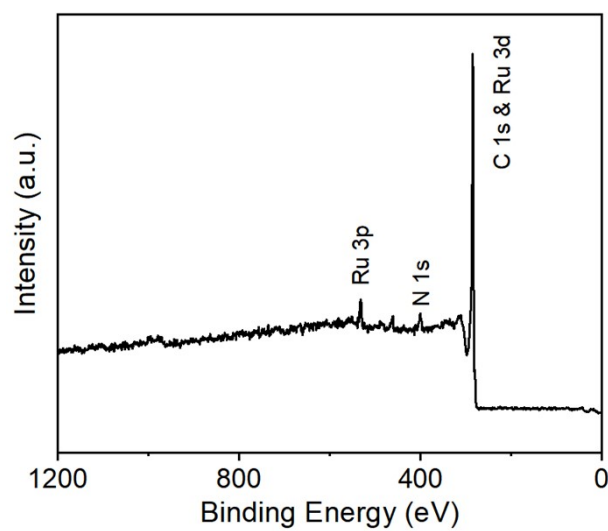


Fig. S6 The full XPS spectrum of Ru_{1+NP8}/NPC.

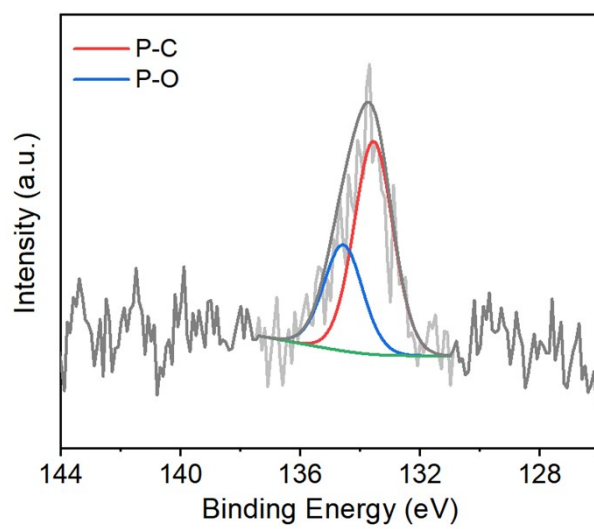


Fig. S7 The P 2p XPS spectrum of Ru₁+NPs/NPC.

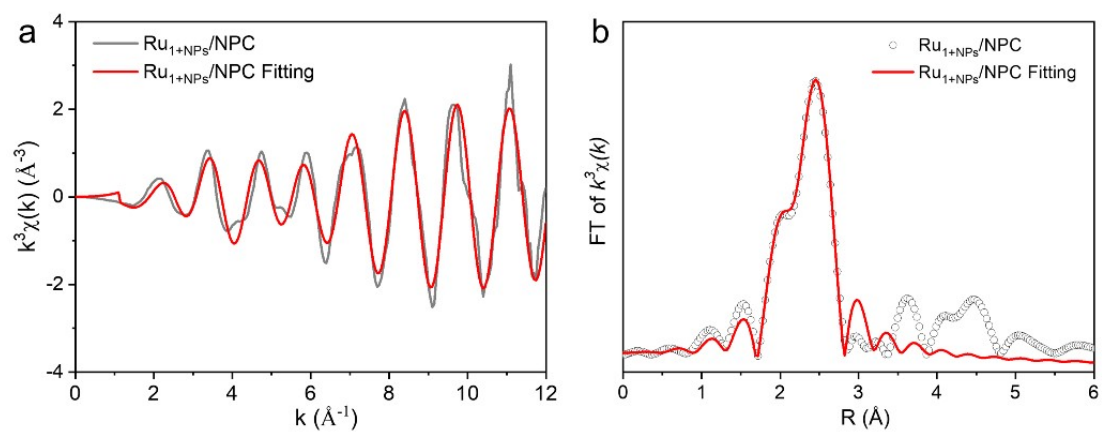


Fig. S8 (a) k space EXAFS of Ru₁+NPs/NPC, **(b)** R space fitting spectra based on the EXAFS of Ru₁+NPs/NPC.

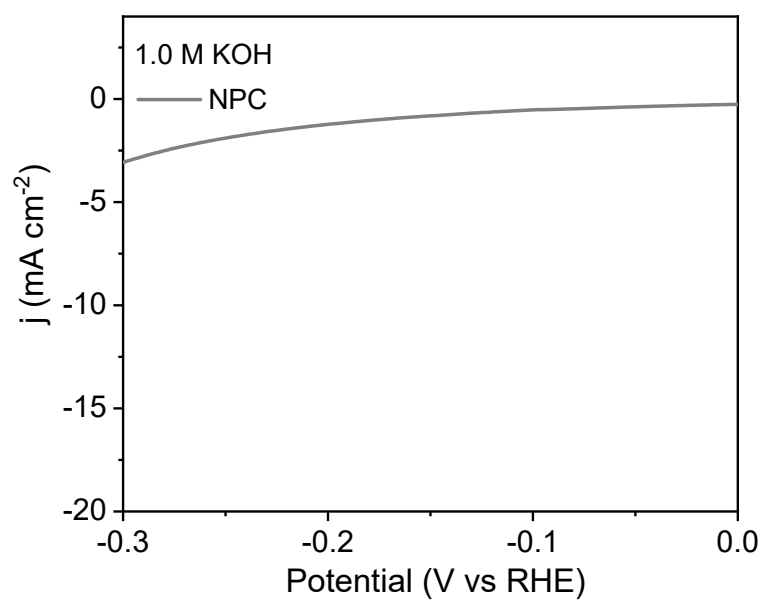


Fig. S9 LSV curves of NPC in 1.0 M KOH.

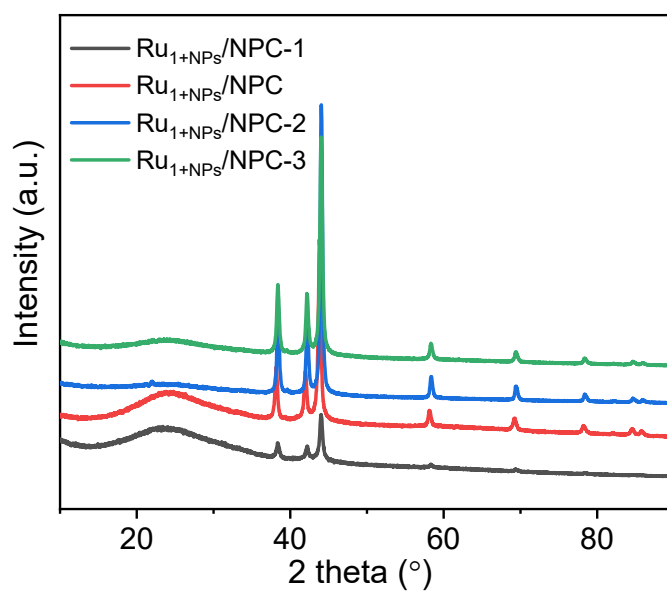


Fig. S10 The XRD patterns of Ru_{1+NPs}/NPC with different Ru contents.

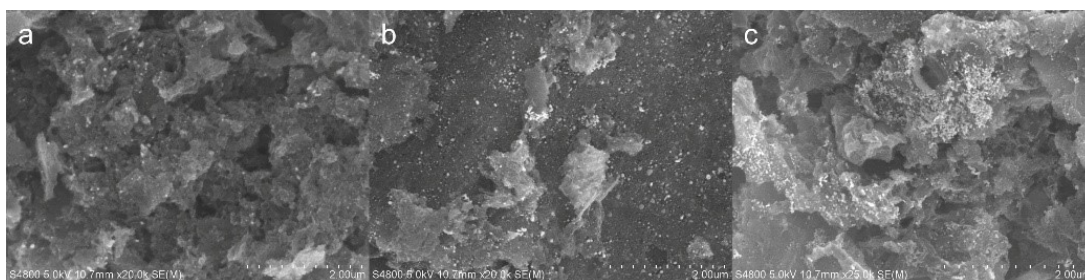


Fig. S11 The SEM images of (a) Ru₁+NPs/NPC-1, (b) Ru₁+NPs/NPC-2 and (c) Ru₁+NPs/NPC-3.

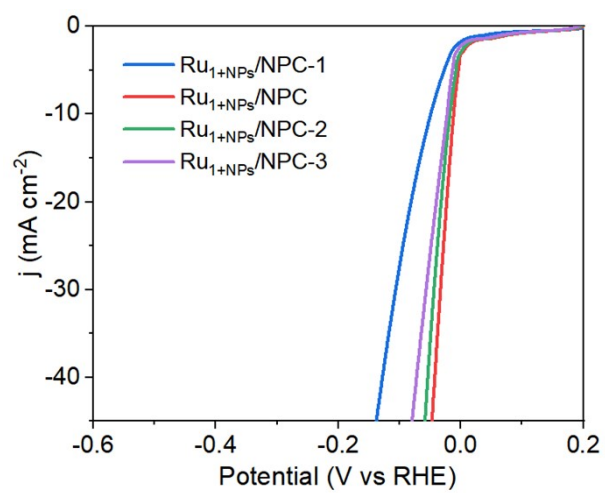


Fig. S12 The HER activities of Ru_{1+NPs}/NPC with different Ru contents.

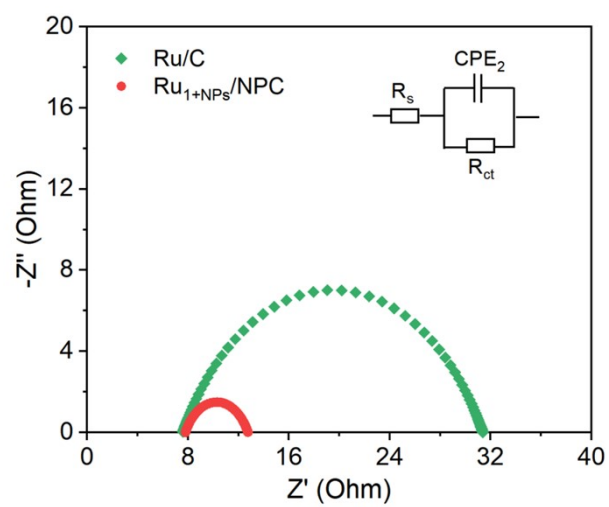


Fig. S13 Nyquist plots of Ru₁+NPs/NPC and Ru/C and fitting equivalent circuit model.

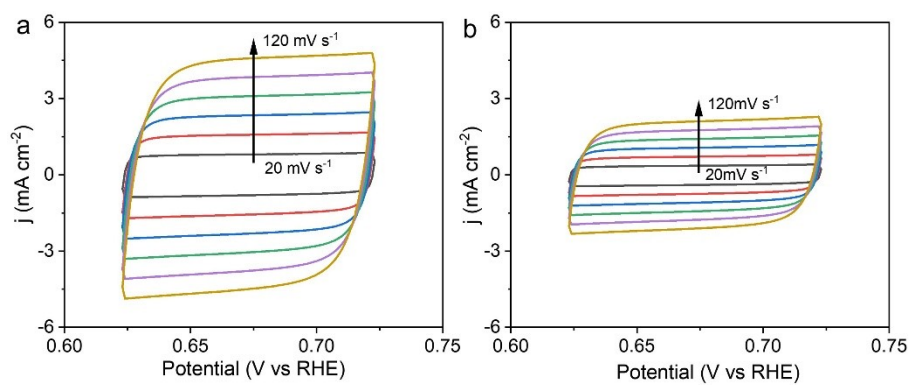


Fig. S14 CV curves of (a) Ru₁+NPs/NPC and (b) Ru/C in alkaline electrolyte at different scan rates.

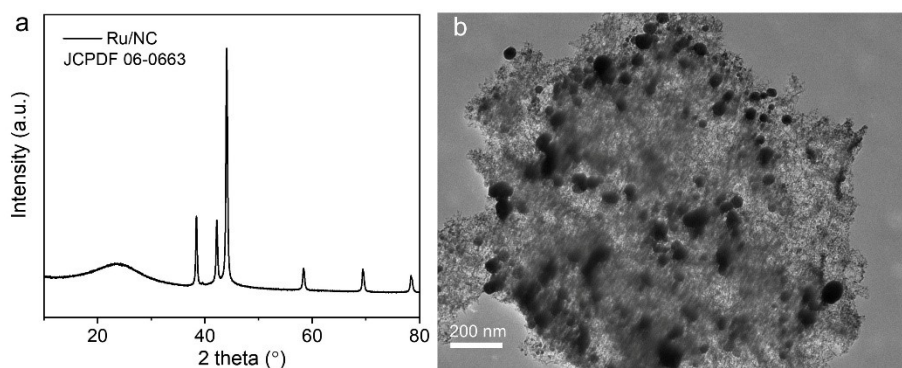


Fig. S15 (a) XRD pattern and (b) TEM image of Ru/NC.

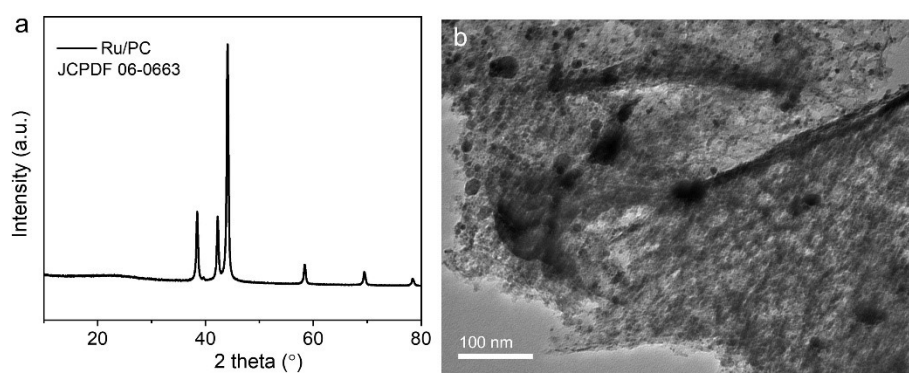


Fig. S16 (a) XRD pattern and (b) TEM image of Ru/PC.

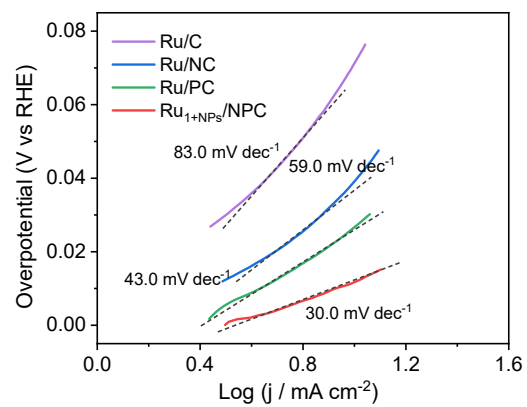


Fig. S17 Tafel slope of Ru_{1+NPs}/NPC, Ru/NC, Ru/C and Ru/PC in alkaline electrolyte.

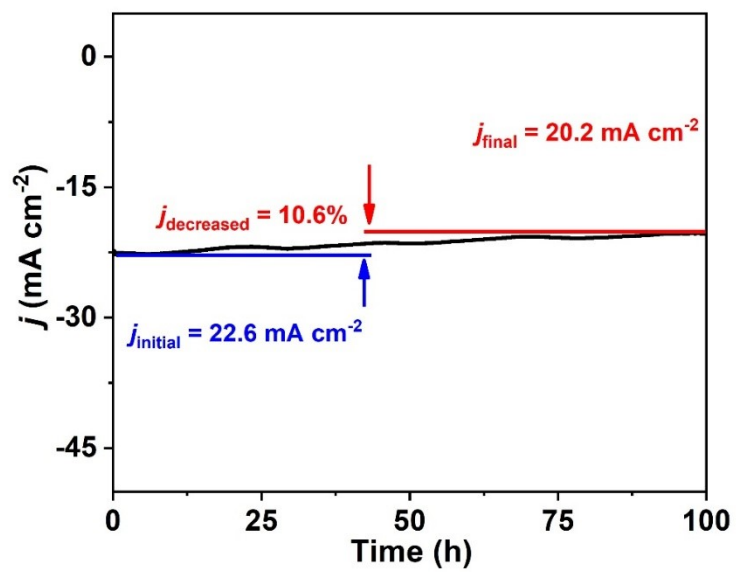


Fig. S18 i - t curve of Ru₁+NPs/NPC after 100 h test in alkaline electrolyte.

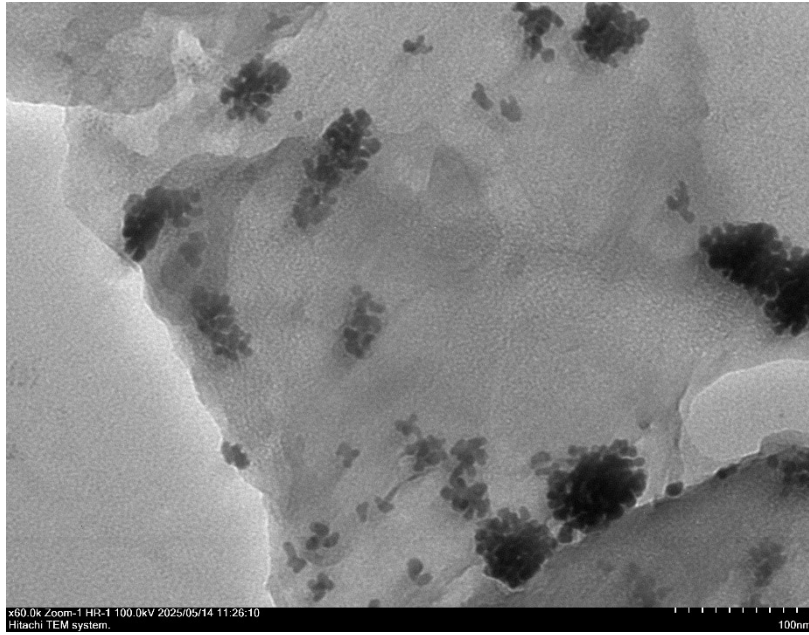


Fig. S19 The morphology of Ru₁+NPs/NPC after 100 h test in alkaline electrolyte.

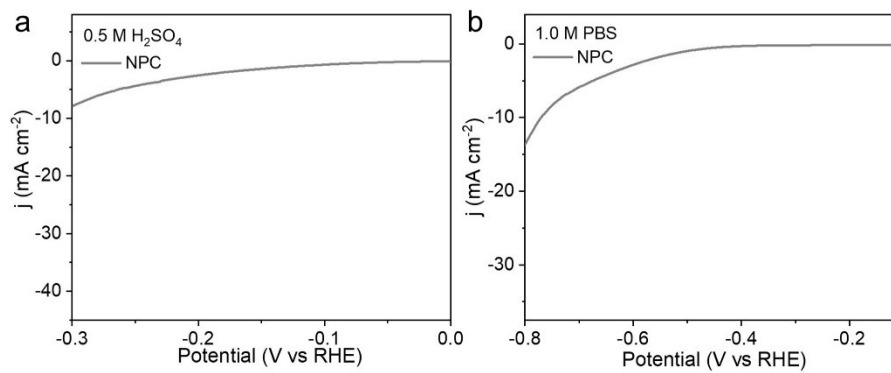


Fig. S20 LSV curves of NPC in (a) 0.5 M H₂SO₄ and (b) 1.0 M PBS.

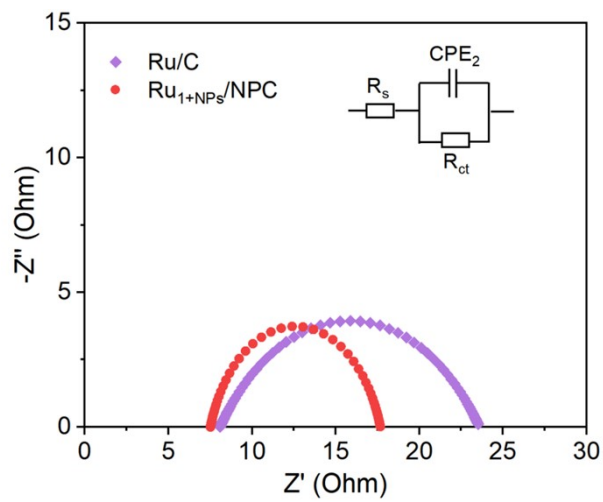


Fig. S21 Nyquist plots of Ru_{1+NP}/NPC and Ru/C in acidic electrolyte.

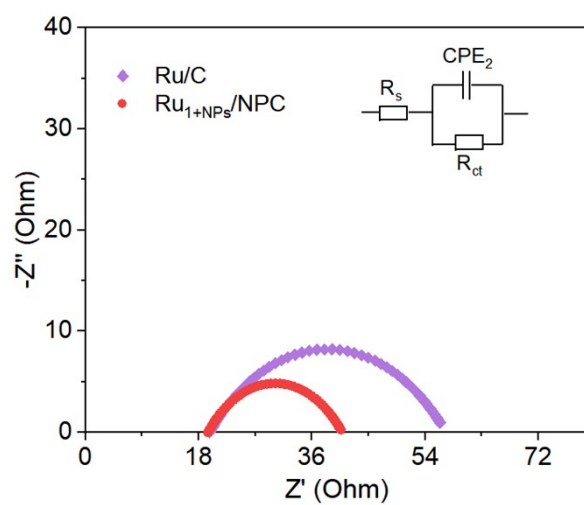


Fig. S22 Nyquist plots of Ru_{1+NP₅}/NPC and Ru/C in neutral electrolyte.

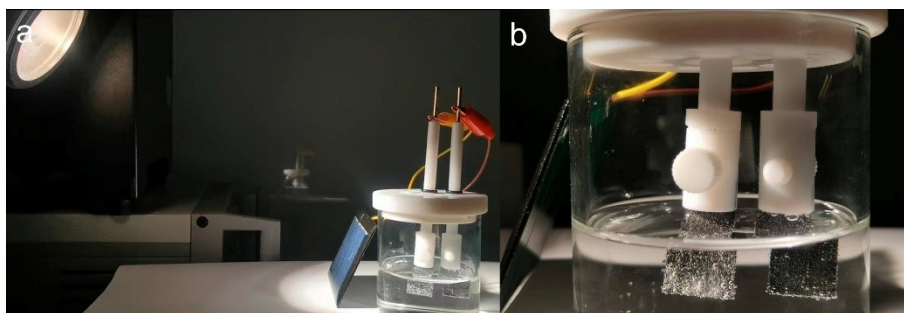


Fig. S23 The photo of $\text{Ru}_{1+\text{NPs}}/\text{NPC}$ II RuO_2 systems was powered by the silicon solar cell in alkaline electrolyte.

Table S1. comparison of HER activities of recently reported Ru based electrocatalysts in alkaline electrolyte.

Catalysts	Electrolyte	@ 10 mA cm ⁻²	Tafel	Reference
Ru_{1+NP}/NPC	1.0 M KOH	12	30	This work
RuO ₂ /NiRu	1.0 M KOH	13	33	J. Mater. Chem. A, 2023, 11, 10720.
Ru-Ru ₂ P@CNFs	1.0 M KOH	14	24.5	Sci. China Mater., 2022, 65, 2675–2684.
NC@RuSA-CoP	1.0 M KOH	15	48.1	Small, 2023, 19, 2301403.
Ru@N-CNfS	1.0 M KOH	17	28.5	Small, 2023, 19, 2206781.
Ru/FNPC	1.0 M KOH	17.8	30	Small, 2024, 20, 2403151
Pt-Ru/RuO ₂	1.0 M KOH	18	18.5	Nat. Commun., 2024, 15, 1447.
RuNP@RuNx-OFC/NC	1.0 M KOH	19	13.75	Appl. Catal. B, 2022, 307, 121193.
C@OV-RuO ₂ /CNTs-325	1.0 M KOH	19.3	39.7	Small, 2024, 20, 2406070
a-Ru(OH) ₃ /CoFe-LDH	1.0 M KOH	20	48.4	Inorg. Chem., 2023, 62, 7424.
P,Mo-Ru@PC	1.0 M KOH	21	21.7	Adv. Energy Mater., 2022, 12, 2200029.
Mo ₂ C-Ru/C	1.0 M KOH	22	25	Adv. Funct. Mater., 2023, 34, 2301925.
Cu-Ru/RuSe ₂	1.0 M KOH	23	58.5	Adv. Mater., 2023, 35, 2300980.
Ru ₂ P/Ir ₂ P HNT	1.0 M KOH	23.2	30.7	Adv. Energy Mater., 2024, 2401426.
Ru NRs/TiN	1.0 M KOH	25	27.08	Appl. Catal. B, 2022, 317, 121796.
Ru/MoSe ₂ @MHCS	1.0 M KOH	25.5	30.2	J. Energy Chem., 2023, 85, 447.
RuFe@NF	1.0 M KOH	28	63.39	J. Mater. Chem. A, 2022, 10, 4817–4824.
Ru/NDC	1.0 M KOH	28.5	20.8	Appl. Catal. B: Environ., 2023, 327, 122466.
RuSe ₂ @NC	1.0 M KOH	30	30	J. Mater. Chem. A, 2022, 10, 7637.
RuP/CN/C	1.0 M KOH	30	40	J. Alloy. Compd., 2023, 939, 168717
Ru-NiCo ₂ S _{4-x}	1.0 M KOH	32	61.3	Adv. Funct. Mater., 2022, 32, 2109731.
MoOx-Ru fcc	1.0 M KOH	34	14.5	ACS Nano, 2022, 16, 14885–14894.
Ru@Ti ₃ C ₂ Tx-VC	1.0 M KOH	35	32	Adv. Energy Mater., 2023, 13, 2300148.
Ru@F-Ni ₃ N	1.0 M KOH	36	52.3	ACS Appl. Mater. Interfaces, 2022, 14, 36688.
CNT-V-Fe-Ru	1.0 M KOH	38	41	ACS Catal., 2023, 13, 49–59.
Ru-G/CC	1.0 M KOH	40	76	Appl. Catal. B, 2022, 317, 121729.
Ru@1T-MoS ₂ -Mxene	1.0 M KOH	42	38	Adv. Funct. Mater., 2023, 33, 2212514.

Table S2. comparison of HER activities of recently reported Ru based electrocatalysts in acidic electrolyte.

Catalysts	Electrolyte	@ 10 mA cm ⁻²	Tafel	Reference
Ru₁+NP₉/NPC	0.5 M H₂SO₄	52	40	This work
MoO _x -Ru fcc	0.5 M H ₂ SO ₄	26	14.5	ACS Nano, 2022, 16, 14885–14894.
RuP/CN/C	0.5 M H ₂ SO ₄	30	60	J. Alloy. Compd., 2023, 939, 168717
C@OV-RuO ₂ /CNTs-325	0.5 M H ₂ SO ₄	36.1	32.8	Small, 2024, 20, 2406070
Ru/MoSe ₂ @MHCS	0.5 M H ₂ SO ₄	38.4	30.3	J. Energy Chem., 2023, 85, 447.
Mo-CoP/Co-N-C	0.5 M H ₂ SO ₄	41	64	J. Mater. Sci. Technol., 2023, 166, 58.
RuSiW	0.5 M H ₂ SO ₄	46	48.9	Adv. Mater., 2024, 36, 2304468
RuSAs@MoSe ₂ -Mxene	0.5 M H ₂ SO ₄	49	52	Carbon, 2024, 218, 118758
Ru-CoP/Ni ₂ P	0.5 M H ₂ SO ₄	53	35.9	Adv. Sci., 2024, 11, 2401398.
Ru/FNPC	0.5 M H ₂ SO ₄	53.8	51.7	Small, 2024, 20, 2403151
Co-Ru/NCN	0.5 M H ₂ SO ₄	62	64	J. Energy Chem., 2023, 87, 286–294
Ru@MoO(S) ₃	0.5 M H ₂ SO ₄	63	32	Nano Energy, 2022, 100, 107445.
Ru/N-CoP-Co ₂ P	0.5 M H ₂ SO ₄	63	46	Inorg. Chem. 2024, 63, 15477–15484
CNT-V-Fe-Ru	0.5 M H ₂ SO ₄	64	51	ACS Catal., 2023, 13, 49–59.
Ru-MoO ₂ /Mo ₂ C/NC	0.5 M H ₂ SO ₄	67	41	J. Alloy. Compd., 2023, 968, 172228.
Br-Ru-RuO ₂ /MCC	0.5 M H ₂ SO ₄	77	49	J. Colloid Interf. Sci., 2023, 646, 391–398.
Ru/CeO ₂	0.5 M H ₂ SO ₄	80	30	J. Colloid Interf. Sci, 2023, 652, 653.
PMO ₁₁ -Ru(acac) ₃	0.5 M H ₂ SO ₄	91	74	ACS Appl. Energy Mater., 2024, 7, 6612–6620

Table S3. comparison of HER activities of recently reported Ru based electrocatalysts in neutral electrolyte.

Catalysts	Electrolyte	@ 10 mA cm ⁻²	Tafel	Reference
Ru_{1+NP}/NPC	1 M PBS	37	49	This work
C@O _v -RuO ₂ /CNTs-325	1 M PBS	18	52.2	Small 2024, 20, 2406070
Ru/FeOx-300	1 M PBS	30	7.3	J. Alloy. Compd., 2025, 1010, 177417
Ru/Nb ₂ O ₅	1.0 M PBS	31	36	Energy Environ. Sci., 2024, 17, 5091.
Ru-PtFeNiCuW/CNTs	1.0 M PBS	34	23.1	Adv. Mater., 2024, 36, 2400433.
Ru-V ₈ C ₇ /C	1.0 M PBS	37	41	Sci. Bull., 2024, 69, 763–771
Ru/RuO ₂ -TiO ₂	1 M PBS	52.7	77.96	J. Mater. Sci. Technol., 2025, 212, 173–181
Ru-O-MoS ₂	1.0 M PBS	54	98	Chem. Sci., 2024, 15, 16281.
RuP/CN/C	1 M PBS	60	76.6	J. Alloy. Compd., 2023, 939, 168717
Ru/WO ₃ -OV	1.0 M PBS	62	81.5	J. Colloid Interf. Sci., 2024, 660, 321–333
Ru-MoO ₂ /Mo ₂ C/NC	1.0 M PBS	67	59.1	J. Alloy. Compd., 2023, 968, 172228
Ru/FNPC	1 M PBS	71.2	60.8	Small, 2024, 20, 2403151
Ru/Ni-NiO/Mo ₂ TiC ₂ Tx	1.0 M PBS	76	68	ACS Appl. Nano Mater., 2023, 6, 22192.
Ru ₃ /Cu-GDYNT	1.0 M PBS	83	60.71	Molecules, 2024, 29, 1410.